THE CONTROL STRUCTURE OF THE NEMATODE *CAENORHABDITIS ELEGANS*: NEURO-SENSORY INTEGRATION AND PROPRIOCEPTIVE FEEDBACK

Charles Fieseler[1*], *James Kunert-Graf*[2] *and J. Nathan Kutz*[3]

[1]Department of Physics, University of Washington, Seattle, WA 98195
[2] Pacific Northwest Research Institute, 720 Broadway, Seattle, WA 98122
[3] Department of Applied Mathematics, University of Washington, Seattle, WA 98195

Word count: 3451 (+318 in captions)

ABSTRACT

We develop a biophysically realistic model of the nematode *C. elegans* that includes: (i) its muscle structure and activation, (ii) key connectomic activation circuitry, and (iii) a weighted and time-dynamic proprioception. In combination, we show that these model components can reproduce the complex waveforms exhibited in *C. elegans* locomotive behaviors, such as omega turns. We show that weighted, time-dependent synaptic dynamics are necessary for this complex behavior, ultimately revealing key functions that must be executed at the connectomic level. Such dynamics are biologically plausible due to the presence of many neuromodulators which have recently been experimentally implicated in complex behaviors such as omega turns. This is the first integrated neuromechanical model to reveal a mechanism capable of generating the complex waveforms observed in the behavior of *C. elegans*, thus providing a mathematical framework for understanding how control decisions must be executed at the connectome level in order to produce the full repertoire of observed behaviors.

1. INTRODUCTION

Of general interest to the biology community is understanding how biomechanical systems process sensory input to produce behavioral outcomes and robust control strategies. Seemingly simple behavioral paradigms such as flying, crawling, and walking all involve complex interactions between neuronal networks of sensory neurons, propioceptive feedback, and muscle activation. Understanding how these various networks interact to produce a robust control strategy remains an open challenge. A model organism that can help elucidate the control laws arising from these complex dynamics is the *Caenorhabditis elegans*: a nematode with only 302 neurons, 95 muscles involved in locomotion, and a well-mapped and stereotyped connectome [1, 2]. Importantly, it has a limited behavioral repertoire that includes four primary motions: forward crawling, backward crawling, omega turns and head sweeps. In this manuscript, we explore a dynamic mechanism that can produce the full repertoire of turns in C elegans in a model optimized for forward motion.

Given its importance as a model organism, there has long been an interest in modeling the behavior and locomotion of the worm (see [4] for a recent review). Broadly, these efforts (i) attempt to model the generation of locomotion within the nervous system alone (e.g. [5, 6, 7, 8, 9, 10, 11, 12]), (ii) model the biomechanics of the musculature/body alone [3, 13, 14, 15, 16, 17, 18, 19], or (iii) build an integrated model for neural and bodily dynamics[20, 21, 22, 23, 24]. Most previous modeling efforts have focused on simulating the simple, sinusoidal bodily postures involved in forward locomotion. It is unclear if said models could be extended to include the more complex behaviors exhibited by the worm. Ultimately, the full complexity of the dynamics may be captured within future high-fidelity, fully three-dimensional particle-based models involving the collaboration of hundreds of scientists and modeling almost every aspect of the *C. elegans* geometry and anatomy [25, 26]. To our knowledge the only model previously shown to be capable of generating complex postures is a non-integrated model of the body alone [3]. This model stops short of considering the role of neuronal dynamics and proprioception in generating complex postures.

Nonetheless, integrated neuromechanical models have generated considerable insight into *C. elegans* locomotion. A notable recent example is the integrated neuromechanical model of Boyle, Berri and Cohen [23], a two-dimensional spring-rod model which uses proprioception to generate sinusoidal locomotion. The model incorporates proprioceptive feedback through specific stretch receptors, which have been long hypothesized [34], and for which there is experimental evidence [33, 34]. Via proprioceptive feedback, the model replicated the experimentally-observed continuous modulation of the worm's forward motion gait in response to its environment [27]. However, this work considered only forward motion, and the model is unable to reproduce other typical behaviors such as backward motion, head sweeps, or omega turns.

In this manuscript, we extend the model of Boyle, Berri and Cohen [23], discovering the necessary modifications for the model to produce the full range of complex *C.elegans* postures. Our modifications produce a single biomechanically realistic model that can produce the full repertoire of behaviors, including the "omega turn" in which the animal makes a deep bend in order to reverse directions. We show that a traveling wave of suppression on the stretch receptors is necessary and sufficient for this complex behavior. This study suggests that transient, extra-synaptic modulation of the synaptic weights is necessary for complex behavior, which is a vital step for understanding the control paradigm of the animal.

2. BIOMECHANICAL MODEL

We review the two-dimensional spring-rod model [23]. This model integrates our dynamic proprioception which generates the repertoire of observed behaviors.

2.1. Environmental properties

This model implements the drag coefficient of the body by separating the parallel and perpendicular components. In relatively low viscosity media similar to water, the drag coefficients can be analytically calculated [36], and in highly viscous media like agar, these coefficients have been experimentally estimated [27, 20]. In the model, the medium is a linearly tunable parameter that varies from 0 (water) to 1 (agar), as shown in table 1.

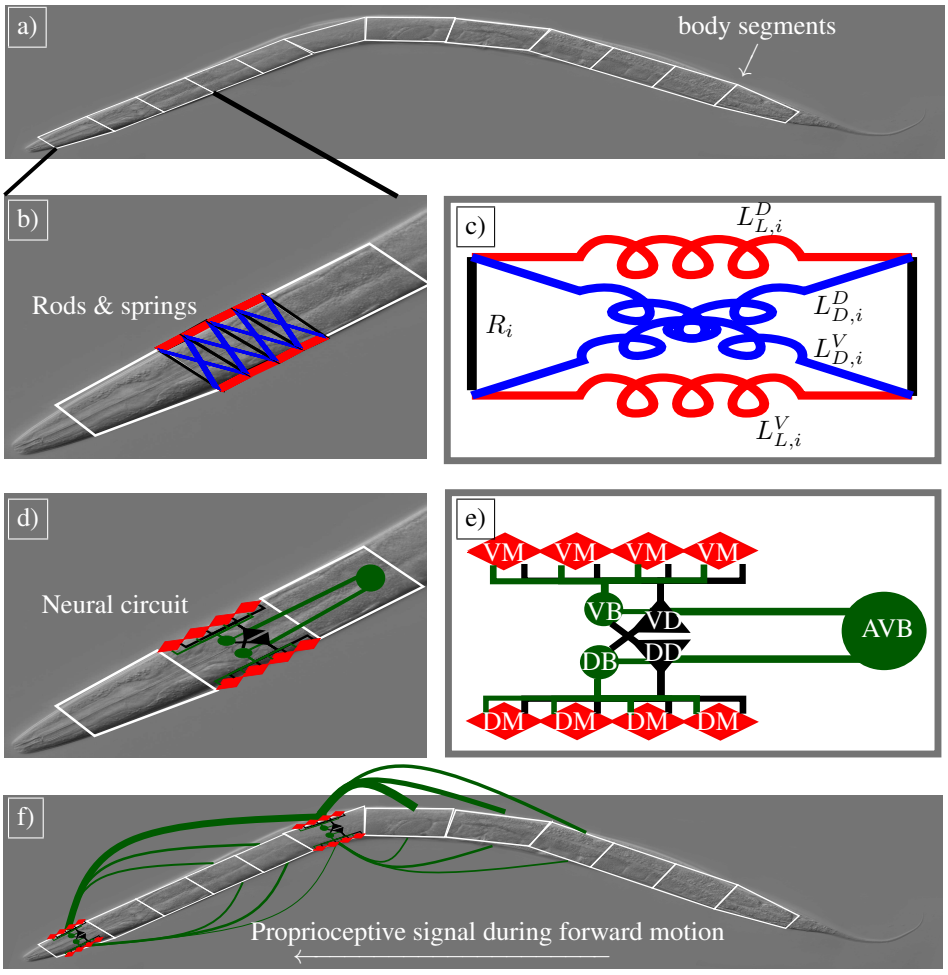

Fig. 1: Biomechanical model of C elegans. Based off of [23]. a) The body has 12 segments. (b) and (c) Each segment has two rigid vertical components and four damped spring components. The diagonal (blue) elements are passive; the horizontal (red) elements are active and controlled by the neuron voltages. d,e) Each segment also has a simplified connectome model, with four pairs of ventral and dorsal motor neurons, and a pair of excitatory B-class neurons and inhibitory D-class neurons. These are activated by a toy "AVB-like" command neuron, for forward motion. f) Proprioception produces oscillation and more complex behavior. A small curvature will produce almost no proprioceptive signaling, but a stretched segment will.

2.2. Model components

The two-dimensional model of the *C. elegans* has long been considered a compromise between feasibility and accuracy [37], i.e. it is a parsimonious model that balances complexity with accurate biomechanics. The two-dimensional structure is motivated by the laboratory environment where nearly the entire body moves only in two dimensions along a surface. The only truly three-dimensional behaviors are exploratory head motions, which are outside the scope of this study.

2.2.1. Body Shape and Segmentation

The *C. elegans* body, as shown in Fig. 1, is composed of 12 segments organized into 3 different layers of interaction. This approximates the known muscle structure: *C. elegans* has 48 dorsal and 47 ventral muscles, though the body itself is not segmented. A segment refers to 8 passive vertical and diagonal elements containing a set of 4 dorsal and 4 ventral muscles, a pair of stretch receptors, and a pair each of A- and B-class neurons. The body is further divided into 48 sub-segments, 4 per full segment, such that each has a pair of lateral, diagonal, and vertical elements and a single muscle.

The two-dimensional cross-section of the body is approximated by an ellipsoid, with the radius of each of the $M = 48$ sub-segments given by:

$$R_i = R_0 \left| \sin\left(\arccos\left(\frac{i - (M/2+1)}{M/2 + 0.2} \right) \right) \right| \qquad (1)$$

where R_i is the radius of the ith body segment and R_0 is maximium radius.

2.2.2. Rod spring model

The first modeling component is a rod-spring system with passive vertical and diagonal elements, as well as active

muscle-driven lateral elements. The vertical rod elements are of a fixed length $2R_i$, given by equation 1, and enforce the biological constraint that the radius of the body is nearly constant throughout normal behavior.

The diagonal elements are damped springs that model hydrostatic internal forces. The force from each diagonal element for the ith body segment is given by:

$$f^k_{D,i} = \kappa_D \left(L_{0D,i} - L^k_{D,i}\right) + \beta_D v^k_{D,i} \tag{2}$$

where β_D and κ_D are the spring and damping constants, and $L_{0D,i} = \sqrt{L^2_{seg} + \left(R_i + R_{i+1}\right)^2}$ is the rest length. In addition, $v_i = \frac{d}{dt} L^k_i$ is the rate of change of the length of each element. The subscripts D and, in the next equation, L, refer to either the diagonal or lateral elements. The superscript k denotes which side of the animal (dorsal or ventral) is being considered and which subnetwork is characterized (A-class or B-class). It can thus take on 4 distinct values. Values are identical across the subnetworks unless otherwise noted. The lateral elements are also damped springs, but these are actively driven by the motor neurons,

$$f^k_{L,\,i} = \begin{cases} \kappa_L \left(L_{0L,i} - L^k_{L,i}\right) + \beta_L v^k_{L,i} \\ \qquad \text{for } \; L^k_{L,i} < L_{0L,i} \\ \kappa_L \left[\left(L_{0L,i} - L^k_{L,i}\right) + 2\left(L_{0L,i} - L^k_{L,i}\right)^4\right] + \beta_L v^k_{L,i} \\ \qquad \text{otherwise} \end{cases} \tag{3}$$

The rest length for the lateral elements is slightly different: $L_{0L,i} = \sqrt{L^2_{seg} + \left(R_i - R_{i+1}\right)^2}$. The force output of a given muscle segment is a function of the motor neuron voltage, the muscle length, and the rate of contraction. In addition, a gradient was imposed on the maximum output force of the muscles, reflecting experimentally observations

$$f^k_{M,i} = \kappa^k_{M,i} \left(L^k_{0M,i} - L^k_{L,i}\right) + \beta^k_{M,i} v^k_{L,i} \tag{4}$$

with

$$\kappa^k_{M,i} \;=\; \kappa^k_{0M} G^k_{NMJ,i}\, \sigma\left(A^k_{M,i}\right) \tag{5a}$$

$$L^k_{0M,i} \;=\; L_{0L,i} - G^k_{NMJ,i}\, \sigma\left(A^k_{M,i}\right) \left(L_{0L,i} - L_{min,i}\right) \tag{5b}$$

$$\beta^k_{M,i} \;=\; \beta_{0M}\, G^k_{NMJ,i}\, \sigma\left(A^k_{M,i}\right) \tag{5c}$$

and where L_{min} is a minimum muscle length for each subsegment, normalized to have the same maximum curvature. The function $G^k_{NMJ,i}$ is a linearly decreasing function from the initiation of the propagation that captures the experimental fact that curvature decreases as the wave propagates. Additionally, $\sigma\left(x\right)$ is a linearized sigmoidal function of the muscle activation:

$$\sigma\left(x\right) = \begin{cases} 0 & , \; x \leq 0 \\ x & , \; 0 < x < 1 \\ 1 & , \; x \geq 1 \end{cases} \tag{6}$$

Parameter	Value
M	48
N	12
L	1mm
$\mathrm{L_{seg}}$	L/M
$\mathrm{CL_{water}}$	$1.65 \cdot 10^{-6} / \left(\mathrm{M}+1\right)$
$\mathrm{CN_{water}}$	$2.6 \cdot 10^{-6} / \left(\mathrm{M}+1\right)$
$\mathrm{CL_{agar}}$	$1.6 \cdot 10^{-3} / \left(\mathrm{M}+1\right)$
$\mathrm{CN_{agar}}$	$64 \cdot 10^{-3} / \left(\mathrm{M}+1\right)$
κ_L	$0.02\ \mathrm{kg \cdot s^{-1}}$
κ_D	$\kappa_L \cdot 350$
κ_{0M}	$\kappa_L \cdot 20$
β_L	$\kappa_L \cdot 0.025\mathrm{s}$
β_D	$\kappa_D \cdot 0.01\mathrm{s}$
β_{0M}	$\beta_L \cdot 100$
$\mathrm{L_{0L,m}}$	$\sqrt{\mathrm{L^2_{seg}} + \left(\mathrm{R_m} - \mathrm{R_{m+1}}\right)^2}$
$\mathrm{L_{0D,m}}$	$\sqrt{\mathrm{L^2_{seg}} + \left(\mathrm{R_m} + \mathrm{R_{m+1}}\right)^2}$
Δ_M	$0.65 \cdot \left(\mathrm{R_m} + \mathrm{R_{m+1}}\right)$
$\mathrm{L_{min,m}}$	$\mathrm{L_{0L,m}} \frac{1-\Delta_M}{2R}$
$\mathrm{R_0}$	$40\mu\mathrm{m}$
ϵ_{hyst}	0.5

2.2.3. Motor neurons

A second critical component of the model is a simplified connectomic structure. In each segment, the pair of 4 muscles receive input from two separate classes of excitatory neurons. These A- and B-class motor neurons form separate subnetworks that are experimentally well-known to be active in backwards and forwards motion, respectively. Each neuron is modeled as bistable neuron which transitions instantanteously and is either "on" or "off," $S = \{0, 1\}$.

$$S^k_i = \begin{cases} 1 & \text{for } \; I^k_i > 0.5 + \epsilon_{hys}\left(0.5 - S^k_n\right) \\ 0 & \text{otherwise} \end{cases} \tag{7}$$

Although there is some evidence that muscles display graded transmission [41], there is also biological evidence for bistability in the worm [42, 32, 31]. Previous work addressing this issue explicitly [23] found no significant difference in behavior when the neurons were modeled using a continuous model of the membrane voltage. The current term is composed of three inputs into each of these motor neurons, given by cross-inhibition, a "command" neuron, and proprioception:

$$I^k_i = w^k_- S^{\bar{k}}_i + I^k_{AVA/AVB} + I^k_{SR,i} \tag{8}$$

The first two terms are explained in detail in the following paragraphs while the third, which contains the key contributions of this work, is detailed in the next section.

In the real worm the contralateral inhibitory GABA-ergic D-class neurons synchronize muscle contractions so that when one side is contracting the other is relaxing. These D-class neurons are connected to the A- and B-class neurons and

their activity is highly correlated. Thus in this model, cross-inhibition is applied directly in proportion to the activity of the excitatory neurons on the opposite side, and is captured in the term $w_{-}^{k} S_i^{\bar{k}}$. The second superscript, $\bar{k}$, refers to the opposite side of the animal (dorsal or ventral).

In the full connectome, these motor neurons are part of larger locomotion circuits and this is modeled here as the second input, from a single *command neuron*. This approximation does not assume that there exists a CPG for the production of oscillatory behavior, but is not incompatible with a hybrid CPG and proprioceptive mechanism. Which (DC) current a neuron receives depends on which subnetwork it is part of, with A-class (backwards) neurons receiving current from the command "AVA," and B-class (forwards) neurons receiving current from command "AVB."

3. PROPRIOCEPTION

We now review the proprioceptive components of the model and introduce our modifications towards a more general dynamic model of proprioception.

3.1. Stretch receptor current

The remaining input (8) into the motor neurons, $I_{SR,i}^{k}$, is also the final component of the biomechanical model: proprioception. Stretch receptors have long been hypothesized to exist due to long, undifferentiated "arms" that extend from the A- and B-class motorneurons down the length of body [34]. Shown in Fig. 1 is how a stretched body segment produces a strong signal for the posterior body segments on the same side, and a weak to non-existent one on the opposite side. The number of segments to be summed over is given by a parameter $s = \min\left(M;\ N_{SR} + (n-1)N_{out}\right)$, which is a constant determined by the number of remaining posterior body segments. The full sum is

$$I_{SR,i}^{k} = (1-\alpha(t)) \cdot A_i \cdot G_{SR,i}^{k} \sum_{j=(n-1)N_{out}+1}^{s} h_j^{k} \tag{9}$$

where

$$A_i = \begin{cases} 1 & ,\ (n-1)N_{out} \leq M - N_{SR} \\ \sqrt{\frac{N_{SR}}{M-(n-1)N_{out}}} & ,\ (n-1)N_{out} > M - N_{SR} \end{cases}. \tag{10}$$

The term $(1-\alpha(t))$ is the time dependent term that allows for dynamic suppression of this current, and will be explained in the next section. The parameter A_i compensates for the fact that for segments close to the posterior of the animal, there are fewer segment contributions. Additionally, the parameter

$$G_{SR,i}^{k} = \begin{cases} 0.65 \cdot \left(0.4 + 0.08 \cdot (N-i-1) \cdot \frac{2N_{seg}}{12N_{seg\ per}}\right) \\ \qquad \text{for } k = A \\ 0.65 \cdot \left(0.4 + 0.08 \cdot i \cdot \frac{2N_{seg}}{12N_{seg\ per}}\right) \\ \qquad \text{for } k = B \end{cases} \tag{11}$$

is a gradient that increases posteriorly for forward motion (B class) and anteriorly for backward motion (A class), to make the receptors more sensitive to the decreased curvature of the body (shown in figure 3). Finally,

$$h_i^{k} = \lambda_i \gamma_m^{k} \frac{L_{L,m}^{k} - L_{0L,m}}{L_{0L,m}} \tag{12}$$

is a stretch receptor activation function with parameters:

$$\lambda_i = \frac{2R_0}{R_i + R_{i+1}} \tag{13}$$

which compensates for the variable radius of each segment with

$$\gamma_m^{k} = \begin{cases} 1 & ,\ k = V \\ 0.8 & ,\ k = D;\ L_{L,m}^{k} > L_{0L,m} \\ 1.2 & ,\ k = D;\ L_{L,m}^{k} < L_{0L,m} \end{cases} \tag{14}$$

which compensates for the previously mentioned asymmetry in the inhibitory circuit. The proprioceptive stretch sensors form the fundamental oscillatory mechanism of the model.

An important note is that proprioceptive feedback for forward motion in our model can be described as an *anteriorly* directed signal encouraging contraction from a *stretched* posterior segment, which is consistent with the physiology of the B motor neurons [1]. In contrast, Quen et al. in [34] provide experimental evidence that proprioception acts as a *posteriorly* directed signal for contraction from a *contracted* anterior segment. It is possible that both of these mechanisms are correct, and possible distinguishing experiments are discussed later in this manuscript.

3.2. Dynamics of proprioception

Unlike simple forward and backward locomotion, which are long-lived oscillations of the network, the omega turn is a transient behavior which only lasts on the order of a few seconds. We phenomenologically model this as a wave of modulation in neuron properties that travels posteriorly along the body. Though the behavior is robust to these details, the functional form used is a two-sided sigmoidal function:

$$\alpha(t) = \frac{1}{2}\left[\tanh\left(s\left(t - t_{start}\right)\right) - \tanh\left(s\left(t - t_{end}\right)\right)\right] \tag{15}$$

where t_{start} and t_{end} are respectively the initiation and completion of wave, and s models the speed at which this suppression takes effect. This function can be used to smoothly tune

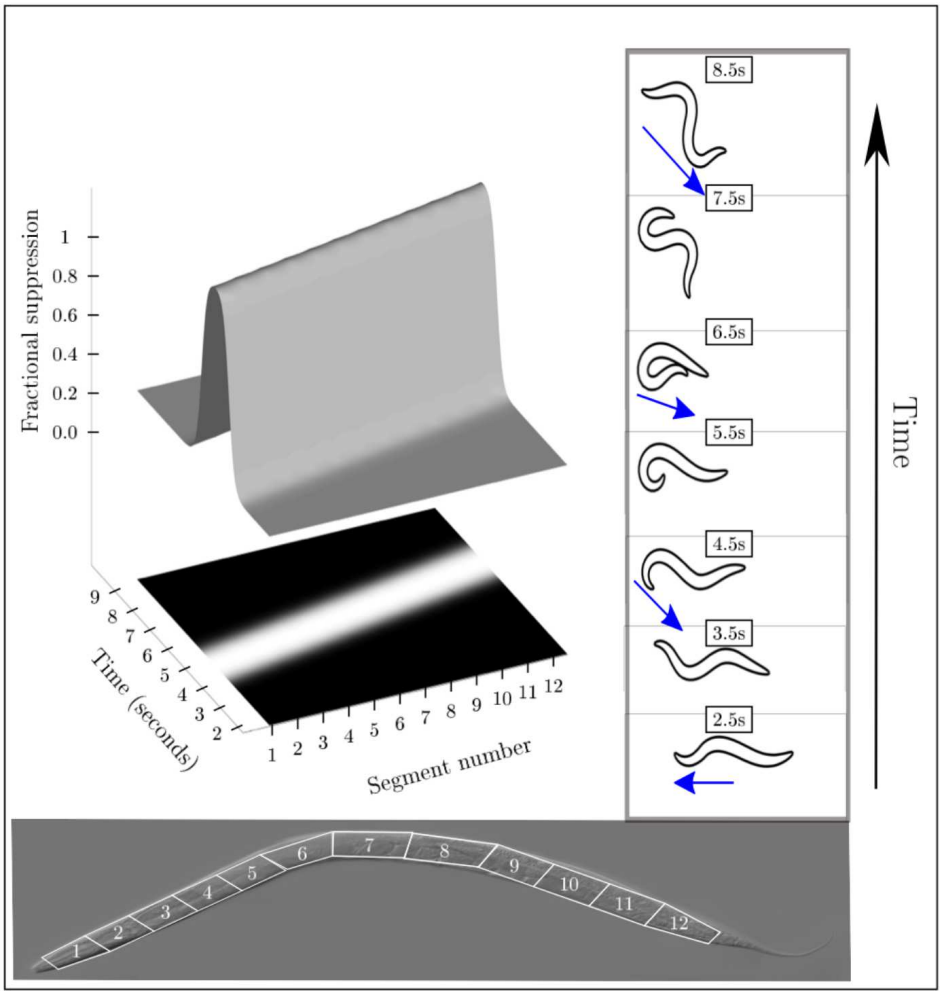

Fig. 2: A wave of suppression on the stretch receptors produces an omega turn. The percent suppressed is shown, which travels along lasting approximately 5 seconds. The snapshots on the right are at the same times as the bold cross sections of the figure on the left.

a parameter to 0 and then back to its full value, as well as increasing or decreasing parameters by a percentage using $1-\alpha$ and $1+\alpha$, respectively. This addition to the original model is vital for complex and transient behaviors like the omega turn and other shallow turns, and is implemented in equation 9.

3.3. Numerical modeling

The original model used Sundials version 2.3.0 [23]; this paper uses version 2.6.1. The numerical simulation portion of the code is written in C++. Based on the original paper, a visualization package written in MATLAB 2016b is included. The model and dynamics proposed here are all fully reproducible, with the code and example datasets openly available at [45]

4. RESULTS

We show our model can produce omega turns and other known behaviors within the model using the dynamics of proprioception.

4.1. Backwards motion

There are three main front-to-back asymmetries that bias the original model towards forwards motion. Two of them are shown in Fig. 3. For forward motion they are: a decrease in muscle strength along the length of the body, and an increase in stretch sensitivity to partially compensate for this.

Importantly, the A- and B-class subnetworks of neurons have "arms" extending in opposite directions down the length of the body [1], and this is modeled as a stretch producing a signal in the anterior body segments for the A neurons. In this way, backwards motion can be plausibly and simply modeled using a mirrored subnetwork of motor neurons with oppositely aligned stretch receptors.

4.2. Optimized stretch receptors

Proprioceptive receptors have long been postulated, but though there are very suggestive experiments [34, 33, 35],

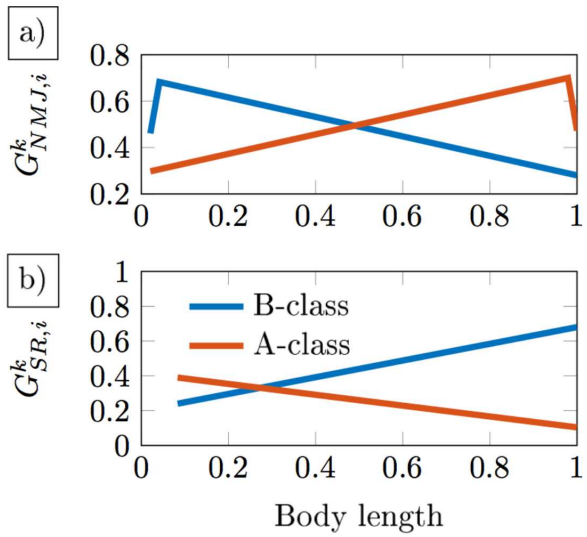

Fig. 3: Asymmetries needed to produce backwards and forward motion. a) The nueromuscular junctions (NMJs) decrease in strength as you travel posteriorly (anteriorly) along the body for forward (backward) motion and B- (A-) class neurons. The head (tail) is weakened in the original model in order to produce straight forward motion, and there is recent experimental evidence that the head circuit is fine tuned in a similar way [46]. b) Partially to compensate for the decrease in NMJ strength, the stretch receptor sensitivity is increased as you travel posteriorly (anteriorly) along the body for forward (backward) motion.

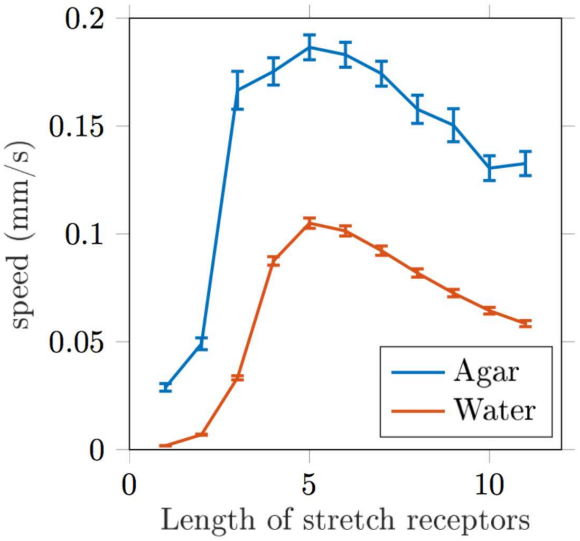

Fig. 4: Average Center Of Mass velocity for regular forward motion as a function of the length of the stretch receptors, measured in body segments.

it is not known through what mechanism the worm senses stretching. Physiological data reveals the presence of long undifferentiated "arms" that stretch away from the B- and A-class motor neurons for approximately a quarter of the body length, but their function is unknown. In order to contribute to constraints on this hypothesis, which is necessary for both simple and complex behaviors in this model, studies on the effect of changing the length of the body receptors on speed of forward motion and other metrics were performed. Figure 4 shows that there is a maximum center of mass velocity for proprioceptive sensors of length equal to approximately 5-6 segments, which would allow each segment to receive information about one half wavelength in agar. The more pronounced feature of figure 4 is the drastic decrease in speed for very short stretch receptors of approximately 1-2 segment lengths.

4.3. Traveling waves of suppression produce omega turns

The addition of a set of parameters that controls a wave of suppression on the stretch receptors along the body wall is enough to realistically produce an omega turn in the model. Figure 2 shows a ventral turn, though this mechanism can produce turns to either side.

In order to understand this behavior, it is instructive to understand what happens to the different body segments as the wave passes through them. When the wave is initialized in the head segment (segment 1), the head becomes less able to sense the curvature of the segments immediately posterior. As the wave travels across the next few segments, the first third of the body continues to tighten its turn because the proprioceptive input is no longer present to stimulate the dorsal muscles, those opposite to those currently active. This tightening continues until the wave passes and the first segments slowly become able to sense the extreme curvature of the first half of the body. The head then starts to unwind, producing a smooth and, depending on the exact parameters, complete change in direction of motion. By tuning the timescale of this wave, the mechanism is able to produce turns of any amplitude.

The continued suppression of the stretch receptors on the posterior half of the body once the head has started to resume normal forward motion is vital to the success of this maneuver. In a realistic omega turn the rest of the body follows the head through the highly curved "omega" shape. This deep bending is resisted by any part of the body in which the proprioceptive signals remain unchanged, something observed in our model (data not shown). Non-traveling suppression of stretch receptors in one part of the body produces various types of thrashing behavior, paralysis, or changes in gait. Furthermore, the forward momentum through the curving head bend must be produced by the continued undulations of the posterior half of the body. Thus, if this proprioceptive hypothesis is correct, a traveling suppression of signals from the stretch receptors is qualitatively necessary.

4.4. Robustness of omega turns

As discussed in [47], a model of a complex system that uses average values of parameters, as this model does, often gives non-average results. Therefore, it is paramount to demonstrate this behavior in an ensemble of models with different internal parameters, and a sensitivity analysis is shown

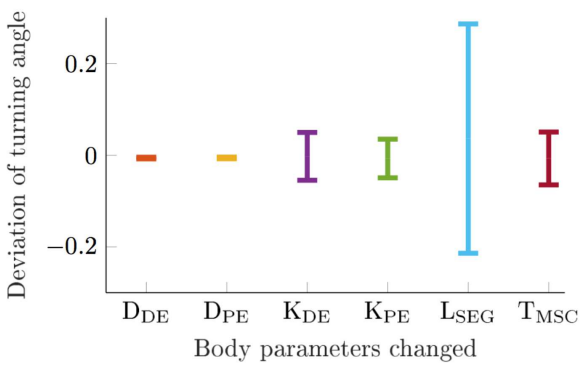

Fig. 5: Angle change as a function of various body parameters. Displayed is the mean and standard deviation when the simulation is run for individuals with up to 10% variation in these parameters: D_*= damping coefficient; k_*= spring constant; $*_{PE}$= horizontal (passive) element; $*_{DE}$= diagonal element; L_{SEG}= segment length; T_{MSC}= muscle time constant.

in Fig. 5. Though the model is relatively sensitive to overall body length, even in this case the turning angle only changed about 0.2 radians, thus suggesting the mechanism is robust in producing omega turns.

5. DISCUSSION

We have presented a biophysically realistic model that can reproduce the essential repertoire of *C. elegans* locomotive behaviors: forward motion, backward motion, head sweeps and omega turns. Recent work has shown that extra-synaptic modulation is important in more complex behavioral patterns in *C. elegans* [38], and this is the first biomechanical model to our knowledge that uses this information and proposes an interpretable mechanism for behaviors beyond forward motion.

This model relies fundamentally on the hypothesis that there exist stretch receptors in *C. elegans*, and that they are posteriorly (anteriorly) directed for B(A)-class neurons. The model further allows for testable predictions about the characteristics of those receptors. Specifically, there must be some type of suppression of the signal sent by those receptors for deep turning behaviors like the omega turn to exist. Mutant studies should be able to identify potential chemical or neural control candidates, which in turn might help illuminate the network involved in proprioception. Another class of experimental tests is through optogenetic manipulation of worms trapped in microfluidic devices along the lines of Quen et al. [34]. If neurons associated with omega turns, e.g. RIV, SMDV, or RIM, are stimulated and a transient down-regulation of the proprioceptive signal is measured, that would be strong evidence for this mechanism.

A traveling wave of modulation, specifically suppression, on the proprioceptive stretch receptors is required to robustly produce omega turns, but we also found that an increase in muscle strength can drastically improve the turning angles of the worm. Though it is possible that the muscle activation is modulated during this behavior, quantitative statements are complicated by many approximations. These issues are discussed in more depth in the original model paper [23]. Thus, unlike the qualitative proposal of a modulatory mechanism on the stretch receptors, no strong quantitative statement can be made about the muscle dynamics themselves.

A general goal of *C. elegans* research is to understand how sensory information is transmuted into behaviors that exist on many different time scales. One step towards understanding this process is through finding the control mechanisms of the neural network that physically cause those behaviors. The ability of a single model to produce all of these behaviors helps elucidate the control structure of *C. elegans*, and can help inform what types of outputs must be produced by the internal dynamics of the network [8]. Omega turns and the type of modulation required to produce them were a critical contribution of this paper. The posited mechanism can also produce much shallower or deeper turns, both of which have been proposed as distinct categories of behavior [43, 44].

Much recent modeling work has contributed to discussions surrounding simple behaviors like forward motion, and we hope that this paper can contribute to similar discussions of more complex behavioral dynamics involving omega turns. Importantly, we have illustrated that dynamic processes can play a critical role in controlling the *C. elegans* repertoire of behavior. In future work, we hope to integrate the connectomic dynamics with the proposed biomechanial model in order to understand the "inside" and "outside" of the worm and how the connectome serves as the controller for behavioral outputs.

Conflict of Interest

The authors declare no conflict of interest associated with this paper.

Acknowledgements

We are indebted to Aravi Samuel for help comments and insights into the *C. elegans* locomotion and dynamics. C. Fieseler acknowledges support from a National Science Foundation Graduate Research Fellowship under Grant No. DGE-1256082.

6. REFERENCES

[1] White, J.G., Southgate, E., Thomson, J.N. and Brenner, S., 1986. The structure of the nervous system of the nematode Caenorhabditis elegans. Philos Trans R Soc Lond B Biol Sci, 314(1165), pp.1-340

[2] Varshney, L.R., Chen, B.L., Paniagua, E., Hall, D.H. and Chklovskii, D.B., 2011. Structural properties of the Caenorhabditis elegans neuronal network. PLoS Comput Biol, 7(2), p.e1001066.

[3] Cohen, N. and Ranner, T. A New Computational Method for a Model of *C. elegans* Biomechanics: Insights into Elasticity and Locomotion Performance. arXiv:1702.04988v1 [physics.bio-ph]

[4] Izquierdo, E.J. and Beer, R.D. 2016. The whole worm: brain-body-environment models of C. elegans. Current Opinion in Neurobiology, 40, pp.23-30.

[5] Niebur, E and Erdös, P. 1988. Computer simulation of networks of electrotonic neurons. In Computer Simulation in Brain Science. Cambridge University Press. pp.148-163.

[6] Sakata, K and Shingai, R. 2004. Neural network model to generate head swing in locomotion of Caenorhabditis elegans. Network, 15, pp.199-216.

[7] Karbowski, J., Schindelman, G., Cronin, C.J., Seah, A., and Sternberg, P.W. 2008. Systems level circuit model of C. elegans undulatory locomotion: mathematical modeling and molecular genetics. J Comput Neurosci, 24, pp.253-276.

[8] Kunert, J., Shlizerman, E. and Kutz, J.N., 2014. Low-dimensional functionality of complex network dynamics: Neurosensory integration in the Caenorhabditis elegans connectome. Physical Review E, 89(5), p.052805.

[9] Portegys, T.E. 2015. Training sensory-motor Behavior in the Connectome of an artificial C. elegans. Neurocomputing,168, pp.128-134.

[10] Kunert, J.M., Proctor, J.L, Brunton, S.L, and Kutz, J.N. 2017. Spatiotemporal Feedback and Network Structure Drive and Encode Caenorhabditis elegans Locomotion. PLoS Computational Biology, 13(1), e1005303.

[11] Kunert, J.M., Maia, P.D., and Kutz, J.N. 2017. Functionality and Robustness of Injured Connectomic Dynamics in C. elegans: Linking Behavioral Deficits to Neural Circuit Damage. PLoS Computational Biology, 13 (1), e1005261.

[12] Kunert-Graf, J.M., Shlizerman, E., and Kutz, J.N. 2017. Multistability and Long-Timescale Transients Encoded by Network Structure in a Model of C. elegans Connectome Dynamics. Frontiers in Computational Neuroscience, 11.

[13] Erdös, P., and Niebur, E. 1990. The neural basis of the locomotion of nematodes. Lect Notes Phys 1990, 368:253-267.

[14] Rönkkö, M., and Wong, G. 2008. Modeling the C. elegans nematode and its environment using a particle system. J Theor Biol 2008, 253:316-322.

[15] Mailler, R., Avery, J., Graves, J., and Wily, N. 2010. Biologically accurate 3D model of the locomotion of Caernorhabditis elegans. International Conference on Biosciences. 2010:84-90.

[16] Majmudar, T., Keaveny, E.E., Zhang, J., and Shelley, M.J. 2012. Experiments and theory of undulatory locomotion in a simple structured medium. J R Soc Interface, 9, pp.1809-1823

[17] Rabets, Y., Backholm, M., Dalnoki-Veress, K., and Ryu, W.S. 2014. Direct measurements of drag forces in C. elegans crawling locomotion. Biophys J, 107, pp.1980-1987.

[18] Backholm, M., Kasper, A.K.S., Schulman, R.D., Ryu, W.S., and Dalnoki-Veress, K. 2015. The effects of viscosity on the undulatory swimming dynamics of C. elegans. Phys Fluids, 27, p.091901.

[19] Lee SH, Kang SH. 2015. Characterization of the crawling activity of Caenorhabditis elegans using a Hidden Markov Model. Theory Biosci, 134, pp.117-125.

[20] Niebur, E. and Erdös, P., 1991. Theory of the locomotion of nematodes: dynamics of undulatory progression on a surface. Biophysical journal, 60(5), pp.1132-1146.

[21] Bryden, J.A., and Cohen, N. 2008. Neural control of Caenorhabditis elegans forward locomotion: the role of sensory feedback. Biol Cybern, 98,339-351.

[22] Boyle, J.H., Bryden, J., and Cohen, N. 2008. An integrated neuro-mechanical model of C. elegans forward locomotion. Lect Notes Comput Sci, 4984, pp.37-47.

[23] Boyle, J.H., Berri, S. and Cohen, N. 2012. Gait modulation in C. elegans: an integrated neuromechanical model. Frontiers in computational neuroscience, 6, p.10.

[24] Deng, X., Xu, J.X., Wang, J., Wang, G.Y. and Chen, Q.S., 2016. Biological modeling the undulatory locomotion of C. elegans using dynamic neural network approach. Neurocomputing, 186, pp.207-217.

[25] Blau, A., Callaly, F., Cawley, S., Coffey, A., De Mauro, A., Epelde, G., Ferrara, L., Krewer, F., Liberale, C., Machado, P. and Maclair, G., 2014, July. The Si elegans Project–The Challenges and Prospects of Emulating Caenorhabditis elegans. In Conference on Biomimetic and Biohybrid Systems (pp. 436-438). Springer International Publishing.

[26] Szigeti, B., Gleeson, P., Vella, M., Khayrulin, S., Palyanov, A., Hokanson, J., Currie, M., Cantarelli, M., Idili, G. and Larson, S., 2014. OpenWorm: an open-science approach to modeling Caenorhabditis elegans. Frontiers in computational neuroscience, 8, p.137.

[27] Berri, S., Boyle, J.H., Tassieri, M., Hope, I.A. and Cohen, N., 2009. Forward locomotion of the nematode C. elegans is achieved through modulation of a single gait. HFSP journal, 3(3), pp.186-193.

[28] Bargmann, C.I., 2012. Beyond the connectome: how neuromodulators shape neural circuits. Bioessays, 34(6), pp.458-465.

[29] Suzuki, M., Tsuji, T. and Ohtake, H., 2005. A model of motor control of the nematode C. elegans with neuronal circuits. Artificial Intelligence in Medicine, 35(1), pp.75-86.

[30] Izquierdo, E.J. and Beer, R.D., 2013. Connecting a connectome to behavior: an ensemble of neuroanatomical models of C. elegans klinotaxis. PLoS Comput Biol, 9(2), p.e1002890.

[31] Gao, S. and Zhen, M., 2011. Action potentials drive body wall muscle contractions in Caenorhabditis elegans. Proceedings of the National Academy of Sciences, 108(6), pp.2557-2562.

[32] Mellem, J.E., Brockie, P.J., Madsen, D.M. and Maricq, A.V., 2008. Action potentials contribute to neuronal signaling in C. elegans. Nature neuroscience, 11(8), pp.865-867.

[33] Li, W., Feng, Z., Sternberg, P.W. and Xu, X.S., 2006. A C. elegans stretch receptor neuron revealed by a mechanosensitive TRP channel homologue. Nature, 440(7084), pp.684-687.

[34] Wen, Q., Po, M.D., Hulme, E., Chen, S., Liu, X., Kwok, S.W., Gershow, M., Leifer, A.M., Butler, V., Fang-Yen, C. and Kawano, T., 2012. Proprioceptive coupling within motor neurons drives C. elegans forward locomotion. Neuron, 76(4), pp.750-761.

[35] Albeg, A., Smith, C.J., Chatzigeorgiou, M., Feitelson, D.G., Hall, D.H., Schafer, W.R., Miller, D.M. and Treinin, M., 2011. C. elegans multi-dendritic sensory neurons: morphology and function. Molecular and Cellular Neuroscience, 46(1), pp.308-317.

[36] Lighthill, J., 1976. Flagellar hydrodynamics. SIAM review, 18(2), pp.161-230.

[37] Izquierdo, E.J. and Beer, R.D., 2015. An integrated neuromechanical model of steering in C. elegans. In Proceeding of the European Conference on Artificial Life (pp. 199-206).

[38] Donnelly, J.L., Clark, C.M., Leifer, A.M., Pirri, J.K., Haburcak, M., Francis, M.M., Samuel, A.D. and Alkema, M.J., 2013. Monoaminergic orchestration of motor programs in a complex C. elegans behavior. PLoS Biol, 11(4), p.e1001529.

[39] Lim, M.A., Chitturi, J., Laskova, V., Meng, J., Findeis, D., Wiekenberg, A., Mulcahy, B., Luo, L., Li, Y., Lu, Y. and Hung, W., 2016. Neuroendocrine modulation sustains the C. elegans forward motor state. eLife, 5, p.e19887.

[40] Haspel, G. and O'Donovan, M.J., 2011. A perimotor framework reveals functional segmentation in the motoneuronal network controlling locomotion in Caenorhabditis elegans. Journal of Neuroscience, 31(41), pp.14611-14623.

[41] Liu, Q., Hollopeter, G. and Jorgensen, E.M., 2009. Graded synaptic transmission at the Caenorhabditis elegans neuromuscular junction. Proceedings of the National Academy of Sciences, 106(26), pp.10823-10828.

[42] Gordus, A., Pokala, N., Levy, S., Flavell, S.W. and Bargmann, C.I., 2015. Feedback from network states generates variability in a probabilistic olfactory circuit. Cell, 161(2), pp.215-227.

[43] Kim, D., Park, S., Mahadevan, L. and Shin, J.H., 2011. The shallow turn of a worm. Journal of Experimental Biology, 214(9), pp.1554-1559.

[44] Broekmans, O.D., Rodgers, J.B., Ryu, W.S. and Stephens, G.J., 2016. Resolving coiled shapes reveals new reorientation behaviors in C. elegans. eLife, 5, p.e17227.

[45] https://github.com/Charles-Fieseler/The-Control-Structure-of-the-Nematode-C-Elegans

[46] Shen, Y., Wen, Q., Liu, H., Zhong, C., Qin, Y., Harris, G., Kawano, T., Wu, M., Xu, T., Samuel, A.D. and Zhang, Y., 2016. An extrasynaptic GABAergic signal modulates a pattern of forward movement in Caenorhabditis elegans. eLife, 5, p.e14197.

[47] Cook, D.D. and Robertson, D.J., 2016. The generic modeling fallacy: Average biomechanical models often produce non-average results!. Journal of Biomechanics, 49(15), pp.3609-3615.